Extension and shear fracturing in the Costa Rica décollement caused by seismically-induced fluid pulsing.

Available online at www.sciencedirect.com
ScienceDirect
Earth and Planetary Science Letters 262 (2007) 413–428
EPSL
www.elsevier.com/locate/epsl

Structural characterization of the Costa Rica décollement: Evidence for seismically-induced fluid pulsing

Paola Vannucchi*, Lorenzo Leoni

Earth Science Department, University of Florence, Via La Pira, 4, 50121 Firenze, Italy

Received 12 January 2007; received in revised form 23 July 2007; accepted 24 July 2007
Available online 14 August 2007
Editor: M.L. Delaney

Abstract

Ocean Drilling Program Legs 170 and 205 offshore Costa Rica provide structural observations which support a new model for the geometry and deformation response to the seismic cycle of the frontal sedimentary prism and décollement. The model is based on drillcore, thin section, and electron microscope observations. The décollement damage zone is a few tens of meters in width, it develops mainly within the frontal prism. A clear cm-thick fault core is observed 1.6 km from the trench. The lower boundary of the fault core is coincident with the lithological boundary between the frontal prism and the hemipelagic and pelagic sediment of the Cocos plate. Breccia clast distributions in the upper portion of the décollement damage zone were studied through fractal analysis. This analysis shows that the fractal dimension changes with brecciated fragment size, implying that deformation was not accommodated by self-similar fracturing. A higher fractal dimensionality correlates with smaller particle size, which indicates that different or additional grain-size reduction processes operated during shearing. The co-existence of two distinct fracturing processes is also confirmed by microscopic analysis in which extension fracturing in the upper part of the damage zone farthest from the fault core is frequent, while both extension and shear fracturing occur approaching the fault core.

The coexistence of extensional and shear fracturing seems to be best explained by fluid pressure variations in response to variations of the compressional regime during the seismic cycle. During the co-seismic event, sub-horizontal compression and fluid pressure increase, triggering shear fracturing and fluid expulsion. Fractures migrate upward with fluids, contributing to the asymmetric shape of the décollement, while slip propagates. In the inter-seismic interval the frontal prism relaxes and fluid pressure drops. The frontal prism goes into diffuse extension during the interval when plate convergence is accommodated by creep along the ductile fault core. The fault core is typically a barrier to deformation, which is explained by its weak, but impermeable, nature. The localized development of a damage zone beneath the fault core is characterized by shear fracturing that appears as the result of local strengthening of the detachment.

Keywords: décollement; fault zone; subduction; Costa Rica; fluid pressure

1. Introduction

Theoretical models of faults are based on geometrical, mechanical and mathematical assumptions; their success at predicting fault behavior is a direct consequence of their ability to match observations (Ben-Zion and Sammis, 2003). Field geologists, however, often find that faults are complex features with laterally varying characteristics, and that fault zone mechanisms and structures appear to be strongly influenced by the interaction with fluids (Sibson et al., 1988; Sibson, 1992; Segall and Rice, 1995).

* Corresponding author.
E-mail address: paola.vannucchi@unifi.it (P. Vannucchi).

0012-821X/$ - see front matter © 2007 Elsevier B.V. All rights reserved.
doi:10.1016/j.epsl.2007.07.056

Fluids shape fault zones by influencing their hydrogeological and mechanical properties. However we still do not know how episodes of fluid flow relate to episodes of fault slip and the mechanisms of fault deformation. Perhaps the most striking and most important examples of fault-fluid interaction come from modern convergent plate margins which have been explored during the Ocean Drilling Program (ODP) activity (Maltman and Vannucchi, 2004, and references therein).

Subduction zones are characterized by the massive fluid release that occurs when the fluid-rich sediments of the incoming plate are either trapped during underthrusting or incorporated into an accretionary prism. When frontal accretion is absent, subduction margins build up a frontal prism formed by fluid-rich sediments reworked from the slope and deposited by gravitational mass movements (Aubouin and von Huene, 1985; Vannucchi and Tobin, 2000; von Huene et al., 2004). The interaction between deformation and fluid flow in subduction zones is not only particularly important along the plate boundary (Bangs et al., 1999; Bangs et al., 2004; Ranero et al., submitted for publication) but also within the upper plate. In the last few years both modeling (Wang and Hu, 2006) and fluid flow measurements on the seafloor and along fault zones within the frontal prism of subduction zones (Morris et al., 2003; Brown et al., 2005) have revealed a dynamic deformation response of the system to the seismic cycle. Here we report on the structural analysis of the Costa Rica décollement drilled near its deformation front by ODP Legs 170 and 205. Here shallow drilling through the décollement has helped to constrain its architecture and the relationship to fluid flow. We will concentrate on the geometrical properties of the décollement to infer the long term – slow – and short term – fast – evolution of the fault and the mechanisms of particle size reduction within the fault zone. We also discuss the deformation pattern of the Costa Rica convergent margin, which has a well developed upper portion of the damage zone and an absent or poorly developed lower damage zone. Asymmetric development of the décollement has important consequences for the gravity driven deformation of the frontal prism and suggests the occurrence of subduction erosion at much shallower levels than previously thought to be feasible (von Huene et al., 2004).

Finally, we investigate the occurrence of pressure transients or fluid discharge associated with slip. Several physical models have been proposed to explain these processes, both seismic and aseismic, as the seismic fault suction-pumping mechanism (Sibson, 2000), and stress changes models in subduction prism (Wang and Hu, 2006). We hypothesize that deformation mechanisms, fluid pressure and composition in the upper plate and in the décollement vary as a response to slip, and also during quiescent period due to fluid–rock interaction and general upper plate relaxation.

2. Costa Rica décollement

The frontal part of the Costa Rica décollement has been drilled four times during ODP Legs 170 and 205 (Kimura et al., 1997; Morris et al., 2003) (Fig. 1). Leg 170 and 205 data constrain a detailed cross section across the décollement. Regionally, the décollement is slipping of 88 mm/yr top to S30°W (DeMets, 2001). The local trend of the décollement is N40°W, and in the shallow portion of interest, geophysical imaging shows a subhorizontal dip (Fig. 1). At ODP Site 170-1043, located ~0.6 km arcward from the deformation front, the complete prism section was cored to 282 m below seafloor (mbsf) in sediment deposited on the Cocos plate. The décollement was identified between 141.50 and 150.57 mbsf, with a total thickness of 15.57 m for the fault zone. The adjacent ODP Site 205-1255, instead, recovered only four drillcores from 123 to 157 mbsf. This limited an accurate location of the top of the décollement, which was tentatively put at 132.7 mbsf, while the base was identified at 144.08 mbsf. ODP Site 170-1040 is located ~1.6 km arcward from the deformation front. Here a complete section of the décollement between 332.6 and 371.2 mbsf was recovered, with the décollement being 38.6 m thick. The adjacent ODP Site 205-1254 also recovered a complete section of the décollement from 319.30 to 367.50 mbsf, that defined a 482 m thick fault zone. Considering displacement and convergence rate the décollements have been respectively active for 6.8 kyr and 18 kyr. The décollement at ODP Site 205-1255 is accompanied by an overlying fault zone with a minimum thickness of 10 m showing the same deformation features of the décollement damage zone (Morris et al., 2003). The décollement zone cuts through a frontal prism formed by clay and silty clay with sand (Fig. 1), that accumulates through mass wasting at the margin toe. Only at ODP Site 205-1254 has deformation also been observed in the upper 5 m of the incoming Cocos plate sediments, which form part of the décollement zone. It is worth pointing out that during ODP Leg 170 the lower limit of the décollement is coincided with the lithostratigraphic boundary between the sediments of the upper and lower plate sections, so that these units were distinguished as “Prism” and “Underthrust” (Kimura et al., 1997). This name designation during ODP Leg 170 was a very unfortunate choice, because in a reference frame fixed to the upper plate, everything from

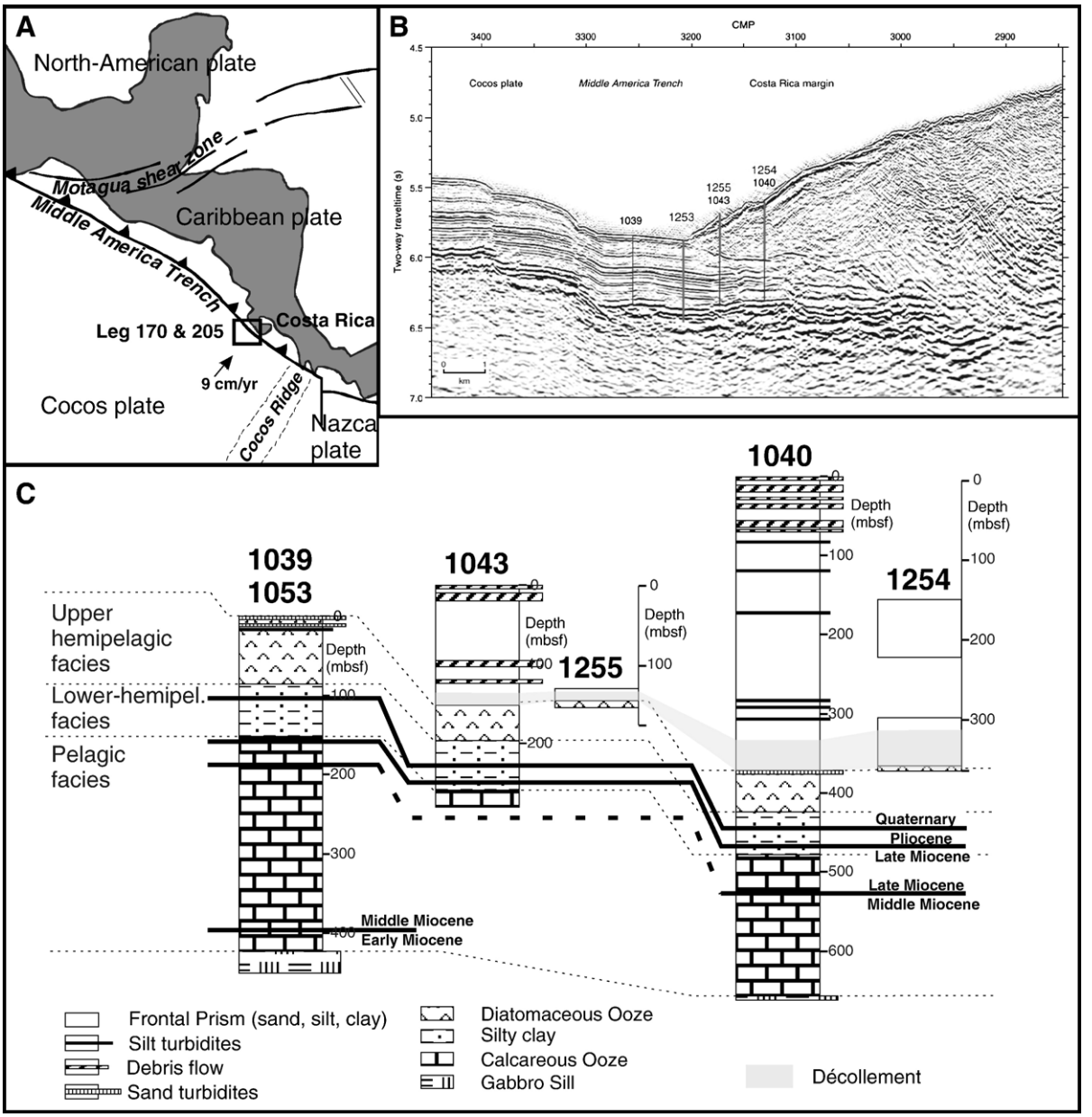

Fig. 1. A) Tectonic sketch of the Middle America Trench. B) A seismic reflection profile shows the locations of ODP Sites 1039, 1252, 1040, 1254, 1043 and 1255. Note the high amplitude of the top-of-prism reflection. Vertical scale indicates two-way traveltime in seconds. C) Correlation of lithostratigraphic units, major time boundaries and décollement within drilled successions of the reference and prism toe sites at this Costa Rica transect.

the top of the décollement zone downward is underthrusting albeit with slower downwards motion than the subducting plate. This is an important point because underthrusting of upper plate material, as described here, indicates that subduction erosion is active at the very frontal part of the margin. For consistency with ODP Leg 170 terminology we will still refer to the Underthrust Unit, meaning the pelagic and hemipelagic sediments deposited on the Cocos plate, so the 5 m dècollement within the sediments of the Cocos plate will still be referred to as being developed within the Underthrust Unit. During ODP Leg 170, drilling of the décollement was characterized by intense drilling disturbance, in particular across the deeper part of the fault where macroscopically the drillcores record ductile deformation in the form of apparent folds and swirled mixing of the silty clay. This fabric, in contrast to the brecciated upper part of the fault domain, was interpreted as being the

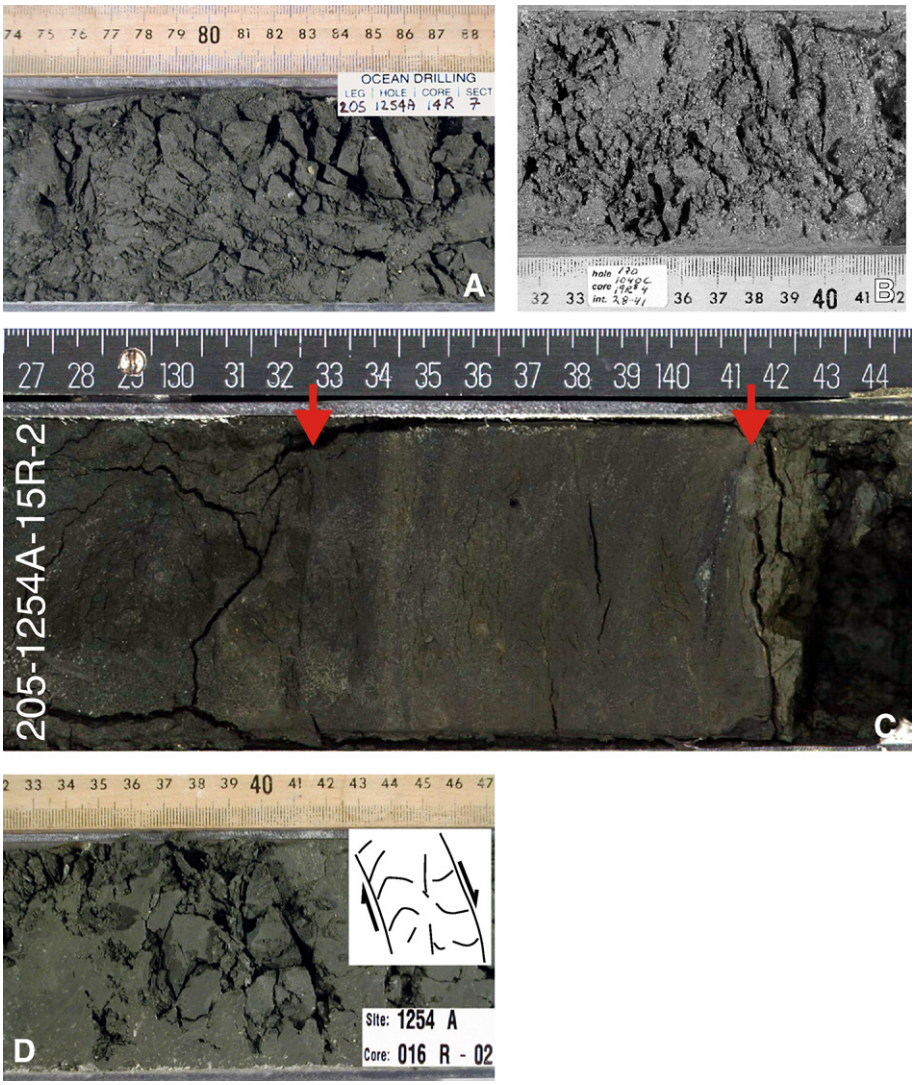

Fig. 2. A) Drillcore photo of the brecciation associated with the décollement deformation in the Prism Unit at Site 1254. B) Drillcore photo of the brittle shear zone associated with décollement deformation in the Underthrust Unit at Site 1254. C) Drillcore photo of the ZLS and the surface of localized slip separating the Prism and Underthrust Units at Site 1254.

response of a different, ductile, local rheology (Tobin et al., 2001). Later, ODP Leg 205 drilling had better quality drillcore recovery across the décollement which revealed that the disturbance was the effect of drilling-induced fluidization of sand lenses causing injections and swirls. The décollement consisted of a brittle damage zone with a ductile fault core/zone of localized shear – ZLS – of just ~10 cm (Fig. 2).

The brittle damage zone can be described as a fault breccia. Deformation has been characterized using clast size classes defined as illustrated in Fig. 3. We will see that the intensity of deformation is proportional to decreasing clast size. Clast sizes generally decrease both toward the lower part of the damage zone as the ZLS is approached, and moving landward from the trench (Fig. 3). The decrease in clast sizes correlates with increasing displacement and confining pressure, the latter mainly controlled by lithostatic pressure. Usually the breccia does not show a preferential fabric, even though as the dimension of the clasts decreases, a foliation oriented at around 60° from the drillcore axis begins to be present in some intervals in addition to a scaly fabric (Fig. 2). The ZLS is localized within the Prism Unit just above the lithological boundary between the Prism and the Underthrust Units, which also coincides with the surface of localized slip. A characteristic of the décollement is a strong deformational asymmetry above and below it (Maltman and Vannucchi, 2004). In fact, in most cases, the displacement pattern

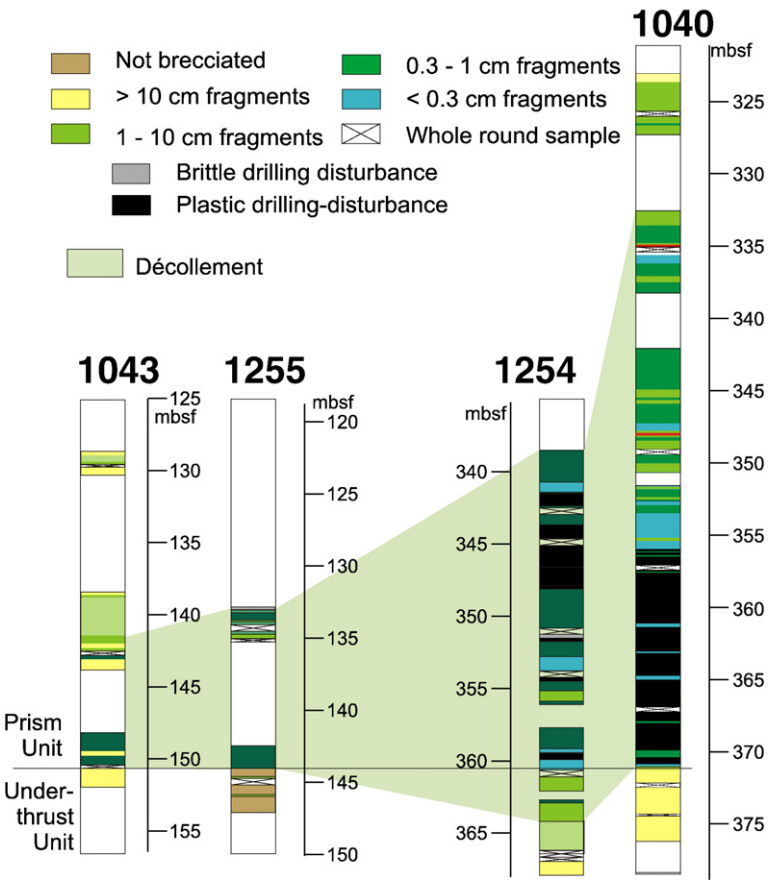

Fig. 3. Details of fracturing across the décollement zone. The density of fracturing is expressed by the nature and size of the brecciated fragments. Note the trend of increasing fracturing landward and downward through the zone. Fracturing peaks above a sharply defined base defined by the lithological boundary between the Prism and Underthrust Units (except for Site 1254 where the décollement encroaches for a short distance within the Underthrust Unit). Leg 170 did not distinguish between 10–3 cm and 3–1 cm classes for this reason and for consistency here we have grouped the two classes, refer to the original figure in Morris et al. (2003) for a more detailed description of Leg 205 brecciation observations.

around the discrete detachment surface has no strain below the décollement surface and a displacement gradient above the decollement surface.

The lithological boundary between the Prism and Underthrust Unit allows us to reconstruct the topography of the décollement, which, considering the degree of vertical error that can be introduced by hole deviations, exhibits a more variable geometry than that imaged seismically, with a basal dip (β-angle) of about 15°.

3. Analysis of fault zone deformation

The geometrical description of the décollement largely depends upon the scale of observation, since the thickness of the damage zone is two orders of magnitude larger than the ZLS, i.e. 10's of m vs. a few cm. Most of the fault slip is concentrated in the narrow ZLS, so that the décollement could be treated as a sequence of planar slip-discontinuities within a deforming continuum solid. Considering the fault breccia, instead we will describe the deformation using a fractal description for granular materials.

Because there are two distinct deformation domains within the Costa Rica décollement, the damage zone and the ZLS, we will first describe each of these domains individually, and then describe their evolution within a conceptual framework of progressive deformation.

3.1. Frontal prism damage zone (Fig. 2A,B)

The damage zone was studied using two different approaches: (1) the analysis of the distribution of clasts within the breccia and (2) microstructural observations in oriented thin sections and scanning electron microscope (SEM) images. Clast size distributions were measured by image analysis of digitized scanned drillcores and direct observations on the sediments. In other words 1) we placed

a transparency directly on each drillcore sampled during the cruise and outlined the clasts, 2) the same samples were photographed with different magnifications, 3) the photographs were digitized, while using the transparencies to help determine individual grains, 4) each digitized image was transformed into a binary (B/W) image in which only the grains are black, and all else is transformed into a white background, 5) The ImageJ-FracLac image analysis software package (Karperien, 2004) was used on each B/W image to determine the particle size distribution. This distribution was calculated with the use of a shifting grid algorithm that does multiple scans from different locations on each binary image, using a non-overlapping sliding-box method. The method calculates several grids of decreasing size that are "placed" over the image. The number of black pixels in each box in the grid is counted for all of the grids. Data are therefore collected for each box of every grid class (for more information on how to analyze digital images and box counting dimension see Karperien, 2004).

The number of particles is then plotted against the corresponding clast size class on a log–log plot (Fig. 4), and the data are parameterized using a power-law function of the form:

$$\log(y) = -D\log(x) + A$$

in which y is the number of particles, x is the clast size, A is a fitting-constant, and D is the fractal dimension, i.e. the slope of the best-fit line (Sammis et al., 1986; Turcotte, 1986). The algorithm finds the average fractal dimension over all scans, as well as a "most efficient" covering fractal dimension. Fig. 4 shows the results from each of these steps. Statistical parameters describing the particle size distribution and power-law best fits are listed in Table 1.

Brecciation in the damage zone produced fractured mudstone and siltstone. We can distinguish intervals with polished fractures that were unaffected or only slightly affected by drilling disturbance. Intervals with injections of soft mud into the fractures are also common. Although we considered them to be natural breccias, we also inferred the presence of artificial matrix material and a superimposed drilling induced fracturation.

For each sample of the damage zone, the number of particles in five clast classes was obtained, namely:>10, 10–3, 3–1, 1–0.3,>0.3 cm. The classes were chosen mainly as an on-board reference as described in Fig. 3 and represent an increasing intensity of brecciation. The Costa Rica décollement cuts through porous detrital sediment. This sediment characteristic suggests the presence of a lower limit for the size of breccia clasts that coincides with the size of the sediment particles and pores, so that the breccia clasts are sediment fragments, while fractures very rarely break down individual sediment grains. When fractures do break grains, the broken particles are in all cases we checked microfossils (Fig. 5A). Thus, the lower limit of clast sizes represents the size where particles can

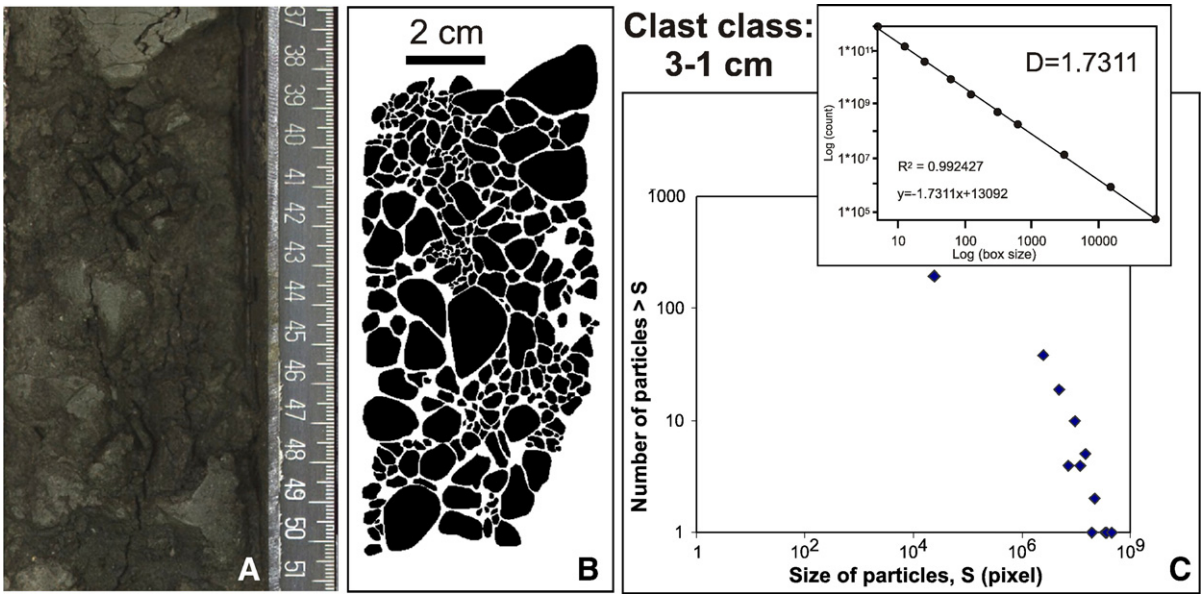

Fig. 4. A) Drillcore scanned photograph of a brecciated interval with clasts of the 3-1 cm class and B) corresponding digitized image. C) Log–log graph showing the numbers of equivalent spherical particles (ordinate) plotted against particle diameters (abscissa) from the sampled cataclastic rocks, and, in the small inbox the best-fit power-law equation and corresponding fractal dimension are also shown.

Table 1
Parameters of particle size distribution and microstructures of sediments in drillcores from ODP Leg 205

Sample	On-board class (cm)	Sediment type	Fracture mode	Fractal dimension	Particle size as measured by image analysis (cm)			Number of particles
					Min	Average	Max	
1254A 12R 02 50–60 cm	10–3	Silty claystone	Mode I	1.65	0.024	1.582	10.280	61
1255A 02R 03 31–45 cm	10–3	Siltstone with clay	Mode I	1.63	0.411	2.639	9.730	32
1254A 14R 07 37–50 cm	3–1	Fine sandstone	Mode I	1.73	0.003	0.122	2.487	282
1254A 14R 07 77–97 cm	3–1	Fine sandstone	Mode I	1.78	0.002	0.729	3.753	334
1254A 15R 01 25–36 cm	1–0.3	Claystone with silt	Shear	1.88	0.0007	0.014	0.748	276
1254A 12R 02 129–139 cm	1–0.3	Silty claystone	Shear	1.85	0.001	0.023	0.632	254
1254A 15R 01 83–88 cm	1–0.3	Claystone	Shear	1.82	0.0004	0,058	0,938	145
1254A 14R 04 120–124 cm	1–0.3	Claystone	Shear	1.86	0,0004	0,084	0,638	159
1254A 15R 02 7–10 cm Thin section	<0.3	Claystone	Shear	1.93	$1.4\ 10^{-5}$	0.002	0,058	448
1254A 12R 02 62–65 Thin section	<0.3	Claystone with silt	Shear	1.98	$3.2\ 10^{-5}$	0.007	0,027	595

be dislodged within pores. These size classes were used as broad categories to sample an equal number of interval so that the error introduced by using these arbitrary classes would be minimized.

The calculated D increases from 1.63–1.65 to 1.93–1.98, in two dimensions, in correlation with the reduction in sizes of the breccia clasts. This indicates that the deformation of the sediment is not accommodated by a self-similar fracturing process.

Clast distribution measurements were taken simultaneously with structural observations on internal fabrics, type of failure mechanism, and evidence for fluid flow within each of the clast-size classes. Textural and X-ray analyses find that clay mineral – smectite – authigenesis is present in the damage zone, as is intergranular cementation (Fig. 6A). Shipboard observations recorded decreasing porosity for the damage zone interval to the base of the frontal prism, with a sharp increase in porosity at the top of the Underthrust Unit (Kimura et al., 1997; Morris et al., 2003). This trend seems contradictory since the frontal prism appears less compacted than the sediment of the Underthrust Unit (Fig. 6B,C). However, early intergranular cementation seems to have developed along the fault zone within the frontal prism. Intergranular cementation would lithify and strengthen the sediment matrix so that it can be then broken and brecciated.

Uncertainties arising from possible drilling-induced deformation are always a potential source of error, so we have tried to be conservative in our drillcore analyses. For example, open and roughly striated fractures oriented at angles ~30° or sub-perpendicular to the drillcore axis have been considered to be potential drilling artifacts. In addition to healed fractures, that are unequivocally in situ features, clear natural fractures are characterized by highly planar surfaces, that occur in parallel sets and do not have an obvious symmetrical relationship to the drillcore axis (Lundberg and Moore, 1986). We also considered fractures filled by comminuted sediments, not drilling mud, to be natural. Because of these technical difficulties we gave highest importance to thin section analysis for defining the nature of fracturing and its relation to orientation.

Analysis in thin sections reveals several types of deformation features. In general it is possible to distinguish extensional from shear-related structures. Extensional structures range from dilation bands to cracks. Shear structures are represented by smooth shear deformation bands and faults, some mineralized. Extension is present throughout the décollement. Non-striated extension fractures (mode I) are visible at the drillcore scale and characteristic of the coarser classes. In thin section and in electron microscope images these fractures are seen as streaks of pores or as calcite cemented veins (Fig. 6D). Even though only a few of the thin sections and SEM chips maintained a good orientation to the drillcore-axis after sample preparation, they commonly show a sub-vertical orientation of the extensional features with respect to the shear bands. Fig. 6E, for example, shows two cross-cutting deformation bands. Their SEM appearance, although similar, differs in the presence or absence of calcite veins. Although there are strongly oriented clay minerals parallel to the walls, these veins do not have shear fibers on their surfaces (see Fig. 6D for comparison) and record a net volume increase that implies extensional opening. This high angle cross-cutting relationship is also maintained in samples that are not so well oriented with respect to the drillcore-axis. Vannucchi and Tobin (2000) also reported two sets of fractures, one sub-parallel and one sub-perpendicular to the drillcore-axis. Dilation bands are common and, like veins, they have widths on the order of 0.1 mm (Fig. 5B). Although irregular in shape most of them are oriented with the

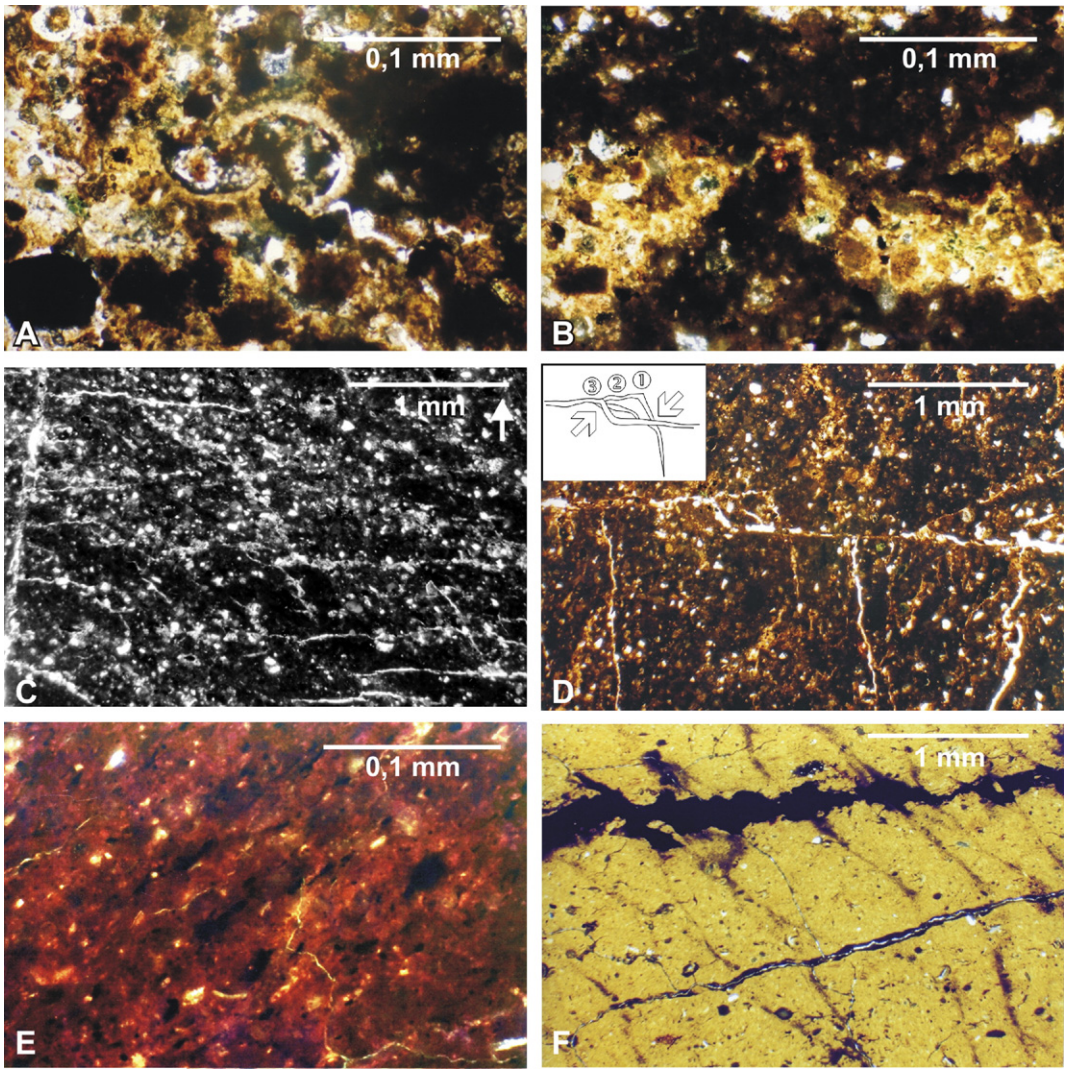

Fig. 5. A) Photomicrograph of a microfault cutting though a microfossil in the damage zone developed in the frontal prism. B) Photomicrograph of a calcite-cemented dilation band in the damage zone developed in the frontal prism. C) Photomicrograph of calcite veins developed in the frontal prism damage zone that are oriented both sub-parallel and oblique to the axis of the drillcore. D) Photomicrograph showing a calcite vein whose trace defines at least 3 opening steps parallel to the top of the photo. Inset: numbering of each increment is based on cross cutting relationships as pointed by the arrows. The vein has an asymmetric distribution of sub-perpendicular calcite veins. Sample from the frontal prism section of the décollement. E) Banded foliation in the fault core. Bands are composed of a very fine grained matrix (<10 μm) with few porphyroclasts. Dark bands are generally, finer grained, and Si–Al-rich (EDAX-SEM analysis) while light bands are coarser grained and more Ca-rich (EDAX-SEM analysis). F) Photomicrograph of en-echelon mud veins cutting through a dark lamina defining bedding in the hemipelagic sediment of the Underthrust Unit of the décollement.

longer axis sub-parallel to the drillcore-axis. Dilation bands typically contain isolated sediment particles from the fracture-wall embedded in calcite cement. The thicker, ~1 mm, dilation bands show a weak gradation with the larger sediment particles clustered together and decreasing in size toward the top, suggesting some degree of sinking of grains in the disaggregated zones. This internal structure suggests slow dewatering through the dilation bands with a flow velocity that was insufficient to prevent sinking of the large particles. As suggested by Knipe (1986a) we can use Stokes Law to estimate the flow velocity from the sinking particle size (~10 μm) and the density (~2.6 g/cm^3) (Kimura et al., 1997). This gives an estimated flow velocity of less than 0.02 mm/sec, i.e.<75 m/yr. This flow velocity, although slow in comparison with the speed of fracture propagation, is 2 orders of magnitude higher than the inferred transient velocity of upward flow along the décollement and 6 orders of magnitude higher than the continuous upward flow velocity would be (Saffer and Screaton,

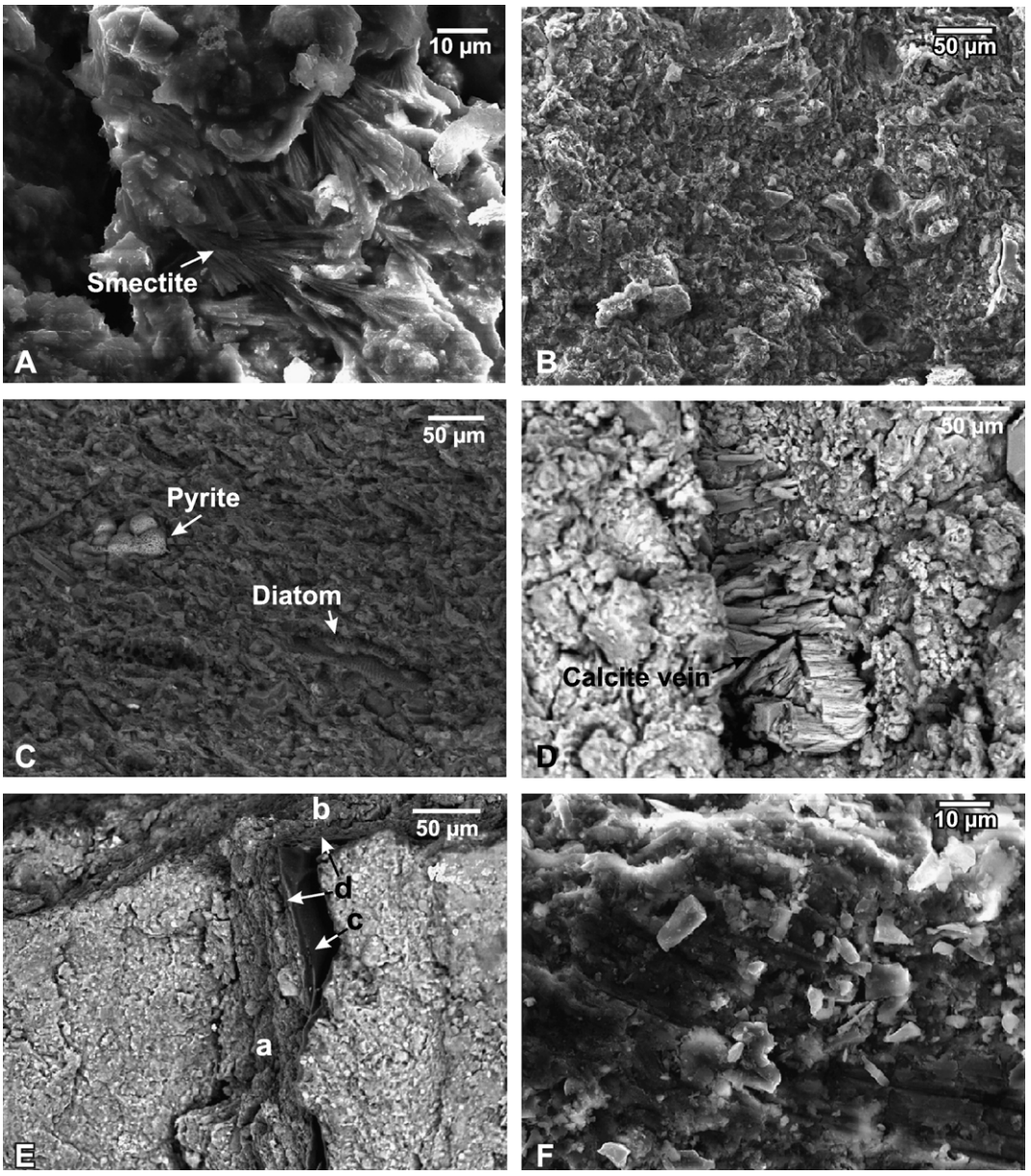

Fig. 6. A) SEM photograph of the authigenic smectite crystals cementing sediment of the prism damage zone. B) SEM photograph of the typical fabric of the sediment involved in the prism damage zone. Note the heterogeneity and the poorly oriented particles, which results in an "open" fabric. C) SEM photograph of the typical fabric of the sediment involved in the damage zone of the Underthrust Unit. Note the high degree of particle orientation and the relatively "close" fabric. D) SEM photograph of an antitaxial, extensional calcite vein in the prism damage zone. E) SEM photograph of a deformation band that is sub-perpendicular to the axis of the drillcore (a) cut by a deformation band sub-parallel to the axis of the drillcore (b). thin calcite veins within the deformation band (c), alternating with well oriented clay layers (d). Here the extensional or shear nature of the veins is unclear, although the lack of fibers typical of shear veins (see Fig. 6D) and the sub-vertical orientation of the vein suggest an extensional opening mode. D) SEM photograph of calcite fibers on the surface of a shear vein.

2003). Particles in the dilation bands do not show evidence of crushing. Band walls also show evidence of shear offsets (Fig. 5B). For this reason, we infer that rotation of particles in the free volume may have occurred, but only as a subordinate process. Dilation without shear is typical of Mode I opening. We infer that the sediments deform with extensional cracks or dilation bands, depending upon the state of consolidation, which is also a function of sediment grain size, cohesion, or effective stress. The cement-supported textures of the dilation bands imply dilatancy and loss of cohesion was accompanied by cementation that occurred at a similar

rate. In SEM images, extension fractures filled by barite are also present. Barite formation appears to be continuous and unidirectional in the direction of fracture opening, with no evidence for multiple events of crack and mineral precipitation. Therefore, fracture opening occurred either at similar (Blenkinsop and Sibson, 1992) or faster rates than did mineral crystallization from the circulating fluid.

Interestingly at this stage of deformation the décollement seems to record only deformation associated with a net volume increase that has no associated porosity collapse. The onset of extensional failure/dilation provides important constraints on the amount and duration of fluid flow and the permeability of the décollement.

Disaggregation records slow background deformation, while extension cracks record faster events, even though subsequent vein-filling precipitation can then occur at a much slower rate.

Shear fractures start to been seen where the breccia clasts reach ~1 cm in size; they become more and more localized as the breccia gets finer grained. With respect to the drillcore axis, shear fractures have either an oblique or sub-perpendicular preferred orientation (Fig. 5C), with striations indicating both normal and reverse senses of displacement along the fractures. At the microscopic scale fractures can occur as shear deformation bands (Fig. 6E), microfaults, or as calcite veins.

Crosscutting relationships show that the shear fractures postdate most of the extensional fractures. It is not possible to deduce clear age relationships between the two sets of shear microfractures oblique and sub-perpendicular to the drillcore axis. However, it appears that the cataclastic process was time progressive, with extensional fractures being the first to form at the onset of sediment brecciation (as they are characteristic of the coarser breccia intervals), with subsequent shear fractures producing ever finer grained breccias.

Calcite and barite crystallization inside the deformation structures indicates the presence of circulating fluids within the damage zone, as can also be inferred from geochemical pore water analyses acquired during drilling (Kimura et al., 1997; Morris et al., 2003). While barite occurs as euhedral crystals filling cavities and extension fractures, calcite is organized in a variety of vein geometries and crystal habits (Fig. 6D,F). Calcite vein geometries vary from almost straight, with symmetrical antitaxial growth, to braided, single crystallization events with no fibers (Figs. 5, 6D). Samples showing vein relationships are uncommon, but the few well preserved ones show distinctive features. Fig. 5D shows a rhomb feature with three preserved dilation stepovers. The veins in the pull-apart show cross cutting relationships that allows the reconstruction of the formation sequence from older (1 in Fig. 5D) to younger (3 in Fig. 5D) events, and indicating that there were three growth episodes across the same surface. The main surface, parallel to the top of photograph, has an asymmetric distribution of veins (see the bottom-right portion of Fig. 5D). Similar structures have been interpreted as evidence for unidirectional stretching or shortening of the rocks associated with slip on the fault (Fletcher and Pollard, 1981). These structures testify to multiple cycles of slip and crystallization along the shear fractures, while there is a general lack of evidence for multiple opening episodes along extension fractures. Therefore the two modes of fracture seems to operate differently and independently along the damage zone.

Shear deformation bands are commonly sites of concentration of fine-grained pyrite crystals indicating the flow of sulfur-rich fluids. The high content of fluids in the sediments is also indicated by ubiquitous spiral drilling-induced deformation patterns. This deformation artifact records injections of sand along the drillcore axis but also shows that fluid saturated sand layers are sealed within clay rich horizons.

3.2. Fault core — Zone of localized shear — ZLS (Fig. 2C)

The ZLS is sharply bounded between the overlying Prism Unit in which the damage zone is mainly developed and the underlying Underthrust Unit. The ZLS is a 10 cm thick layer of gouge with no evidence of mesoscopic fracturing (Fig. 2C). Deformation is ductile, with cm to mm thick color bands sub-perpendicular to the drillcore axis and parallel to the ZLS edges. At a microscopic scale the banded fabric appears to be composed of a very fine grained matrix, <10 μm, with few porphyroclasts, in which the dark finer grained bands are rich in Si and Al, while the light coarser grained zones are rich in Ca (Fig. 5E). The bands define a foliation where grains are mainly flattened and sheared, with only a small contribution from oriented growth. The sediment mainly deforms by compaction associated with grain reorganization and, in some cases, additional sliding and rotation. Intragranular strain and particulate flow seem to be the primary deformation processes, even though microscopic features also record the presence of microfracturing and veining (Fig. 5E). Unlike the fractures and veins developed within the damage zone that are a few mm to cm long, the fractures in the ZLS are sub-mm in thickness. Again, we avoid the possibility of misinterpreting drilling-induced features by restricting our observations to fractures filled by calcite. These veins do not have a clearly symmetrical growth of

calcite, so that it is not possible to interpret them unambiguously as either shear or extensional fractures.

3.3. "Underthrust Unit" damage zone (Fig. 2D)

The characteristics of the well compacted Underthrust Unit are described in Vannucchi and Tobin (2000). ODP Leg 170 drilling across the Costa Rica décollement showed that the sharp surface of localized slip was also the boundary between the deformed frontal prism section and the undeformed Underthrust Unit (Kimura et al., 1997). ODP Site 205-1254, instead, is characterized by the transfer of deformation into the Underthrust Unit, composed of Cocos plate sediments. At the drillcore scale deformation is indicated by ~5 cm thick bands arranged in the form of brittle shear zones that are sub-perpendicular to the drillcore axis (Fig. 2D). In the upper 3 m brittle shear zones are almost continuous; their frequency decreases toward the bottom leaving undeformed portions of drillcores. Paleomagnetic measurements allow the reorientation of the drillcores to establish the sense of shear, which is consistently top to the SW, consistent with the large scale subduction geometry.

Thin section analysis reveals systems of parallel shear deformation bands, microfaults, and en-echelon mud veins usually less that 1 mm thick (Fig. 5F). Shear deformation bands are characterized by the alignment of platy phyllosilicates into the band orientations. Microscopic shear deformation bands that define a spaced foliation were described in the Underthrust Unit sediments recovered at ODP Leg 170 (Vannucchi and Tobin, 2000). Sampling at Site 205-1254 reveals the presence of mud veins associated with deformation bands. Mud veins were not previously observed at Costa Rica sites, but are common at other drilled convergent margins, especially in slope sediments (Knipe, 1986b). Mud veins are commonly arranged in an en-echelon tension-gash geometry with sense of shear well in agreement with the structural onset of brittle shear zones. Mud veins do not have visible displacement associated with them and different sets of veins mutually cross cut each other which suggests that the strain associated with each vein is small and transient. Brothers et al. (1996) showed that mud veins are the result of partial liquefaction produced by the passage of shear waves in a porous sediment characterized by a high degree of grain interlocking. Brothers et al. (1996) conducted their experiments on diatomites, a sediment very similar to that of the Underthrust Unit in Costa Rica (Kimura et al., 1997; Morris et al., 2003). The occurrence of the mud veins in the flat lying Underthrust Unit suggests that they were generated during the passage of seismic shear waves.

4. Discussion

4.1. Fractal analysis

Analysis of the clast size distribution within the brecciated damage zone reveals a not self-similar geometry. Although the fractal dimensions are consistent for each size-class, the overall analysis indicates that brecciation was not a self-similar process. This lack of self-similarity has also been observed in other fault zones, for example in the strike-slip Mattinata Fault (Storti et al., 2003; Billi and Storti, 2004). In the Costa Rica décollement the fractal dimension D of the 10–3 cm class is very close to the $D=1.6\pm0.1$ measured in several cataclasites (Sammis et al., 1986; Sammis et al., 1987; Sammis and Biegel, 1989; Chester et al., 1993). Sammis et al. (1987) modeled the particle size distribution corresponding to $D=1.6\pm0.1$ and proposed a generation mechanism in which clasts may break depending upon the relative size of their nearest-neighbor clasts. This process, called "constrained comminution" to indicate that fragmentation occurs under high confining pressure, visualizes a particle as being most fragile when loaded by neighbors of similar size, since this geometry produces a bipolar load and maximum tensile stress within the particle (Sammis et al., 1987; Ben-Zion and Sammis, 2003). Constrained comminution leads to a final distribution in which each clast has neighbors of different sizes at any scale. The coarser breccia of the damage zone is characterized by extension fractures where no shearing been observed, in accordance with the fact that this part of the damage zone seems to accommodate only a minor portion of the displacement across the décollement.

Extension fractures commonly develop at low confining stress and/or low differential stress. These conditions did not seem to occur in the damage zone, furthermore the particle size distribution implying a process of "constrained comminution" suggests that fracture occurred under high confining pressure. However, high fluid pressure can nucleate extensional fracture even at great burial depths. Pervasive fluid flow is inferred from geochemical pore water analyses acquired during drilling (Kimura et al., 1997; Morris et al., 2003) and local fluid overpressure can be related to the permeability structure and the type of co-seismic deformation. The general sub-vertical trend of the extensional features implies a sub-vertical maximum principal stress, σ_1. Alternating phases of horizontal and vertical σ_1 across the Costa Rica frontal prism were described by Vannucchi and Tobin (2000). Temporal changes in basal friction can generate this alternating

stress pattern, with sub-vertical σ_1 (coincident with the lithostatic stress) recording a phase of low friction along the décollement and relaxation of the prism (Wang and Hu, 2006). Furthermore, extension cracks form rapidly in comparison to dilation bands, especially in the wet clay-rich sediments of the frontal prism , even though subsequent vein-filling precipitation can occur at a much slower rate. While quantifying the rupture velocity is beyond the scope of this paper, we can qualitatively discriminate between fast and slow deformation events.

Approaching the ZLS, brecciated horizons are characterized by particle size distributions with a higher fractal dimension D. This implies that either a different or an additional particle reduction process operates during intense shearing (Fig. 7). Although this result may be partially biased by the clast sizes becoming more and more visible relative to the size of the drillcore, this is a common strain evolution in cataclasites since the fracturing process of constrained comminution becomes saturated at a relatively small amount of total strain (Ben-Zion and Sammis, 2003). During this evolution, fault slip becomes localized along a dominant surface—the ZLS. The fractal progression observed in fault breccias has been interpreted in several ways: (1) as evidence for multiple fracturing events (Blenkinsop, 1991); (2) as the effect of increasing confining pressure and energy input (Engelder, 1974); or (3) as relict surfaces that are not participating in slip localization (Ben-Zion and Sammis, 2003). The transition from a single tensile fragmentation to shearing and comminution has also been invoked based on experimental data (Grady and Kipp, 1987), but this process would only explain the transition from lower fractal dimensions to $D=1.6\pm0.1$, while in the Costa Rica décollement $D=1.6\pm0.1$ is the initial measured value. A fracture process leading to even higher D values for the characteristic particle size distribution has been proposed by Turcotte (1986), but his "plane of fragility" model, where failure occurs by a plane of fragile domains, is a static model that does not correspond to a clearly defined dynamic process.

4.2. Deformation pattern within the décollement zone

The main character of the drilled Costa Rica décollement is the strong asymmetry of deformation toward the upper plate, here composed of a sedimentary frontal prism.

The analysis of the Costa Rica décollement indicates that two competing processes, cataclasis and particulate flow, accommodate the total displacement. In the damage zone, where cataclasis is well developed, extensional failure and disaggregation appears to predate shearing, and tends to become more common as one approaches the ZLS (Fig. 7). In the ZLS particulate flow is well developed, with only minor fracturing.

Shearing occurred only in part on already-formed fractures, and evidence for shear failure is also common. In all cases shear deformation is always on the order of a few mm. Drillcore analysis confirms the small displacements of shear events. The fractal fracturing process seems to have accommodated no significant shear component of the total slip along the décollement.

The upper damage zone of the décollement can be viewed as a transitional zone, in which the stress regime of the upper plate is progressively overprinted by the

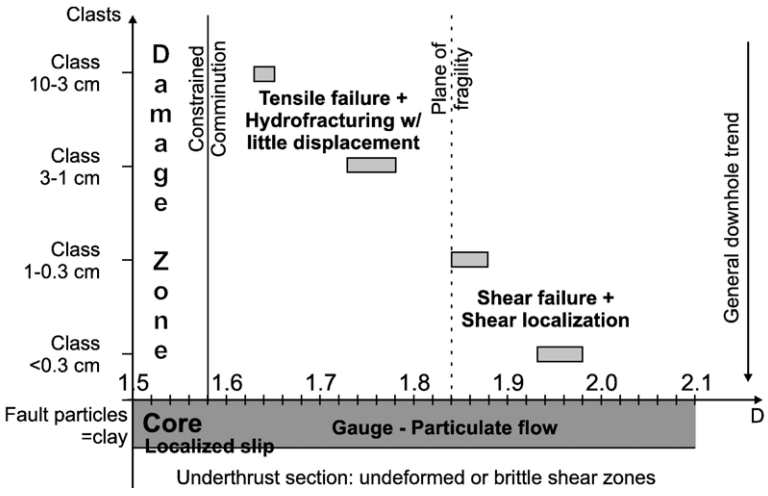

Fig. 7. Summary of the deformation processes active on the Costa Rica décollement that are indicated by meso-microscopic observations. Fractal dimensions are shown for the prism damage zone.

shear stress associated with subduction slip, the latter becoming fully developed only with the gauge of the ZLS. In this view the upper plate's stress regime contributes to the development of the décollement as recorded in the décollement damage zone.

Migration of the décollement deformation into the upper plate and consequent underthrusting is consistent with the erosive nature of the Costa Rica margin (Vannucchi et al., 2001; von Huene et al., 2004). This observation indicates that subduction erosion is even active at the very frontal part of the margin. Interestingly the accretionary Nankai margin also has a shallow portion of the décollement that shows asymmetric strain distribution toward the upper plate (Maltman and Vannucchi, 2004). Recent modelling by Wang and Hu (2006) suggests that basal erosion along the frontal part of the margin can occur in response of simultaneous high basal friction and high pore pressure. The same authors suggest that this combination is unlikely to be present across the entire outer wedge, but can transiently occur in local patches during great earthquakes.

A second implication for the Costa Rica margin is that the frontal prism is an ephemeral feature that behaves as a dynamic mass, i.e. subject to changes in stress/strain state with time. The frontal prism appears to be particularly sensitive to pressure transients or fluid discharge pulses associated with slip events (Brown et al., 2005). In this view the presence of a frontal prism can work to both elevate pore fluid pressure and decrease fault friction (von Huene et al., 2004) allowing for continuous creep along the ZLS, and, since it is part of the outer wedge that is forced to slip during great earthquakes (Wang and Hu, 2006), it can also trigger velocity strengthening reactions and increase basal friction.

At most drilled sites the deformation stops along the décollement with the ZLS. This indicates a complete detachment of the Underthrust Unit. In the case of Site 205-1254 deformation is transferred into the Underthrust Unit. The reason for the transfer of deformation to the Cocos plate sediment of the Underthrust Unit is not obvious from the recovered drillcore. We can speculate either a possible geometric cause, from a flat-ramp geometry to the décollement, or perhaps this occurred during strain localization events driven by fluid overpressure that may episodically overshoot a small distance beyond the basal décollement.

4.3. Fluid behavior

Fluids are abundant in this deforming region (Saffer and Screaton, 2003; Screaton and Saffer, 2005; Davis and Villinger, 2006). In addition, to further confirm this fact, the existence of pervasive veining also provides a record of changes in fluid pressure. Hydrofracturing, though possible, cannot be clearly documented here.

The damage zone cutting through the frontal prism show mineralized fractures that imply the existence of at least two different behaviors for fluid pressure. Dilation bands and the continuous calcite growth in the extensional failure domain do not show obvious evidence for cycles of fluid pressure. Most of the deformation occurred after failure, so these observations imply a slow development to maintain the continuous texture of the observed band and vein fillings. The lack of crack-seal patterns or other evidence for discontinuous growth imply that each structure is the result of a single deformation event. In the shear fracture domain the occurrence of mineralized veins and dilational stepovers indicates that each vein event was produced by an episode of slip on the shear surface followed by fracture healing. This evolution can be described as a type of stick-slip behavior (Davison, 1995) indicating that even at shallow depths there is a fluid cycle where the fluid pressure can drop enough to precipitate calcite. Continuous growth of the veins within the dilation stepover is also unlikely, because, similar to a crack-seal sequence, each event would open one crack producing a surface of weakness that would absorb all the slip of the fault.

Although there is evidence for a fluid cycle within the drilled portion of the décollement, the frontal prism overlies the up-dip velocity-strengthening part of the subduction fault. This is also indicated by the increasing thickness of the ZLS with increasing displacement. Nonetheless the presence of fracturing and extreme localization indicates that the ZLS deforms by different mechanisms through time, which could imply some degree of strain-softening. This same behavior can be seen in the structures of the ZLS of the Nankai décollement from Site 131-808 (Maltman and Vannucchi, 2004). There deformation bands are cut by sharp surfaces indicating extreme slip localization events.

4.4. Frontal prism and shallow décollement zone in earthquake cycle

The increasing thickness of the ZLS with displacement indicates that strain-hardening is active as the first order deformation process. Nevertheless the décollement zone as a whole records different deformation features indicating both its transitional nature and the presence of alternating stress regimes, i.e. upper plate-localized slip. The qualitative discrimination between fast and slow events indicates that some elastic stress is supported along the décollement. The record of stick-slip behavior

along the shear fractures also suggests cycles of fluid pressure implying the presence of suction-pumping mechanisms during fracturing (Sibson, 2000).

These processes can be linked to the stress changes within the frontal prism during the earthquake cycle (Wang and Hu, 2006). Their model illustrates how during an earthquake the subduction fault is forced to slip so that the frontal prism is pushed into a compressional critical state where basal and internal stresses increase as does the fluid pressure. After the seismic event the subduction thrust is required to slip to dissipate the coseismic stress, at the same time the frontal prism relaxes and the fluid pressure drops. The sub-vertical σ_1 of the extensional phase is coincident with the lithostatic stress, in agreement with this recording a phase of relaxation of the prism generating the conditions for the continuous and slow development of the deformation features. In this case relaxation would follow the co-seismically generated stress in the prism (Wang and Hu, 2006).

Fig. 8 shows the proposed model for cyclic behavior of deformation that is implied by the observations presented here. During a co-seismic event, the sub-horizontal compressional stress increases in the wedge as does fluid pressure (Wang and Hu, 2006). The rise in fluid pressure triggers fracturing and fluid expulsion, during which both extensional cracks and shear fractures develop in the damage zone. Fracturing migrates upward with fluid migration, now involving the undeformed section of the frontal prism, and contributing to the typical asymmetric form of the décollement, while slip propagates along localized patches. After the seismic event the frontal prism relaxes and fluid pressures drop. The frontal prism goes into a mode of diffuse extension recorded by the formation of dilation bands. If fractures are not healed by mineral precipitation, then they can also progressively open. At the same time convergence during inter-seismic periods occurs via continuous slip along the ductile ZLS. We also infer that, as a consequence of this relaxation, the ZLS can collapse under the weight of the frontal prism generating an overpressure. The local overpressure and the low permeability of the ZLS cause small fractures to develop.

An implications of this mechanism is that the fluid pressure within the fault zone will vary not only as a response to slip, but also during quiescent periods due to fluid–rock interaction and ZLS gouge compaction. This mechanism can also trigger fluid exchange with the lower damage zone and underthrust section that can affect the composition of the pore fluid (Saffer and Screaton, 2003).

The Underthrust Unit from ODP Leg 170 showed mesoscopically undeformed sediment, while in thin section it displayed deformation bands that can be interpreted as seismically induced dehydration features. There fractures opened and closed without liquefaction (Vannucchi and Tobin, 2000). In the lower damage zone at ODP Site 205-1254, mud veins indicate the presence of liquefaction and clay migration filling the open voids is induced by co-seismic deformation within the sediment.

5. Conclusions

The Costa Rica décollement deforms in a brittle deformational regime where extensional and shear fracture

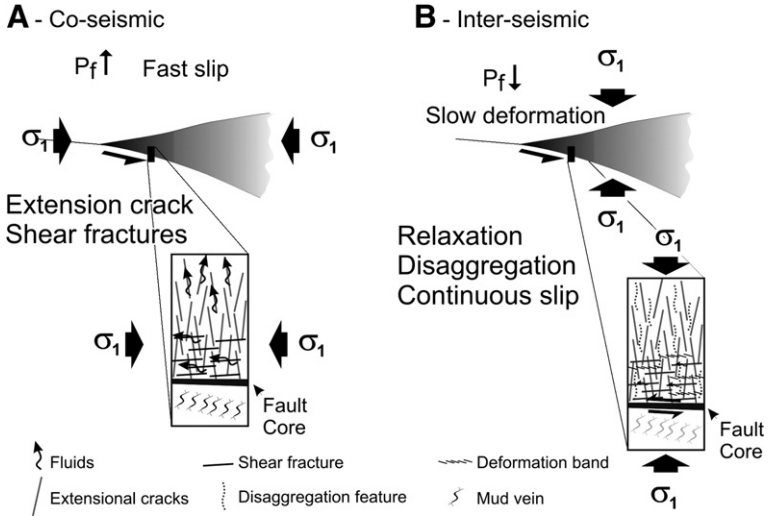

Fig. 8. Conceptual model for the deformation along the Costa Rica décollement during the seismic cycle.

co-evolve with the fluid system. Yet the distributions of particle size reductions imply an increasing amount of shear toward the zone of localized shear, in agreement with increasing displacement, and extensional fractures as precursor evidence of fault damage. The abrupt change in texture between the breccia of the damage zone and the gouge of the zone of localized shear suggests an abrupt spatial change in the magnitude of shear strain. The damage zone, with its particle size distribution following typical fractal laws, seems to have accommodated no significant shear strain beyond that associated with its initial formation. Thus most of the 1.6 km of slip occurred along the narrow ~10 cm-wide zone of localized shear. Although this structural analysis suggests a general strain-hardening behavior of the fault, shear localization also occurred at the early stages of fault development.

The zone of localized shear is typically a "barrier" to the transfer of shear deformation to the pelagic and hemipelagic Cocos plate sediment forming the Underthrust Unit. The presence of a complete detachment is best explained by the existence of pervasive high fluid pressures in the zone of localized shear that maintain its persistent structural weakness. This interpretation agrees with geochemical data illustrating that the zone of localized shear is a barrier to fluid flow with very little fluid passing through this zone, while in contrast the fractured damage zone of the frontal prism is a preferential conduit for fluid flow (Kimura et al., 1997; Morris et al., 2003; Screaton and Saffer, 2005). At ODP site 205-1254 some deformation was transferred beneath the zone of localized shear indicating localized strengthening of the detachment surface and the possibility of localised fluid exchange between the downgoing and overriding plate.

The behavior observed in the frontal prism appears to be a direct consequence of the high fluid content in the décollement. The Costa Rica décollement, although presumed to be aseismic in its drilled portion, contains a record of transient high fluid overpressures evidenced by early-onset cementation and fracturing events. The alternating development of fast and slow deformation and the cyclical nature of fracturing suggests there are transient stress regimes composed of intervals of stable creep along the décollement and stress-relaxation within the upper plate, sandwiched between intervals of sudden compression of the upper plate that follow major slip event followed by an increase in basal friction (Fig. 8). The sudden slip generated strain hardening of the outer wedge and frontal prism can, in this high fluid environment, also produce local fluid overpressure. As a consequence, it can also trigger shallow and localised tectonic erosion (Wang and Hu, 2006).

Acknowledgements

We are grateful to Francesca Remitti for reading and Jason Phipps Morgan for helping in improving an early version of the ms. All shipboard participants to ODP Leg 205 were precious companions, in particular PV thanks Demian Saffer for sharing the duty of drillcore description. Harold Tobin was a great help from onshore. This research has been funded by PRIN 2005 *Cyclic distributed vs. localized deformation and seismic signature in subduction-related fault zones* to G. Molli and PRIN 2005 *Subduction complex dynamics: mass transfer in fossil systems and comparisons with modern examples* to E. Pandeli.

References

Aubouin, J., von Huene, R., 1985. Summary: Leg 84, Middle America Trench transect off Guatemala and Costa Rica. Initial Reports, DSDP, 84. V. H. R. and J. Aubouin. Government Printing Office, Washington, D.C., U.S, pp. 939–956.

Bangs, N.L., Shipley, T.H., Gulick, S.P.S., Moore, G.F., Kuromoto, S., Nakamura, Y., 2004. Evolution of the Nankai Trough decollement from the trench into the seismogenic zone: inferences from three-dimensional seismic reflection imaging. Geology 32 (4), 273–276.

Bangs, N.L.B., Shipley, T.H., Moore, J.C., Moore, G.F., 1999. Fluid accumulation and channeling along the northern Barbados Ridge decollement thrust. J. Geophys. Res. 104 (B9), 20399–20414.

Ben-Zion, Y., Sammis, C.G., 2003. Characterization of fault zones. Pure Appl. Geophys. 160, 677–715.

Billi, A., Storti, F., 2004. Fractal distribution of particle size in carbonate cataclastic rocks from the core of a regional strike-slip fault zone. Tectonophysics 384 (1–4), 115–128.

Blenkinsop, T.G., 1991. Cataclasis and processes of particle size reduction. Pure Appl. Geophys. 136, 59–86.

Blenkinsop, T.G., Sibson, R.H., 1992. Aseismic fracturing and cataclasis involving reaction softening within core material from the Cajon Pass drill hole. J. Geophys. Res. 97 (B4), 5135–5144.

Brothers, R.J., Kemp, A.E.S., Maltman, A.J., 1996. Mechanical development of vein structures due to the passage of earthquake waves through poorly-consolidated sediments. Tectonophysics 260 (4), 227–244.

Brown, K.M., Tryon, M.D., DeShon, H.R., Dorman, L.M., Schwartz, S., 2005. Correlated transient fluid pulsing and seismic tremor in the Costa Rica subduction zone. Earth Planet. Sci. Lett. 238, 189–203.

Chester, F.M., Evans, J.P., Biegel, R.L., 1993. Internal structure and weakening mechanisms of the San-Andreas Fault. J. Geophys. Res. Solid Earth 98 (B1), 771–786.

Davis, E.E., Villinger, H.W., 2006. Transient formation fluid pressures and temperatures in the Costa Rica forearc prism and subducting oceanic basement: CORK monitoring at ODP Sites 1253 and 1255. Earth Planet. Sci. Lett. 245 (1–2), 232–244.

Davison, I., 1995. Fault slip evolution determined from crack-seal veins in pull-aparts and their implications for general slip models. J. Struct. Geol. 17 (7), 1025–1034.

DeMets, C., 2001. A new estimate for present-day Cocos–Caribbean plate motion: Implications for slip along the Central American volcanic arc. Geophys. Res. Lett. 28 (21), 4043–4046.

Engelder, J.T., 1974. Cataclasis and the generation of fault gouge. Geol. Soc. Amer. Bull. 85, 1515–1522.

Fletcher, R.C., Pollard, D.D., 1981. Anticrack model for pressure solution surfaces. Geology 9 (9), 419–424.

Grady, D.E., Kipp, M.E., 1987. Dynamic rock fragmentation. In: Atkinson, B. (Ed.), Fracture Mechanics of Rocks. Academic Press Inc, London, pp. 420–475.

Karperien, A., 2004. FracLac Advanced User's Manual. Charles Sturt University, Australia, p. 36 (http://rsb.info.nih.gov/ij/plugins/fraclac/fraclac.html.).

Kimura, G., et al. (1997). Proceedings of the Ocean Drilling Program, Initial Report, 170. College Station (TX), Ocean Drilling Program.

Knipe, R.J., 1986a. Faulting mechanisms in slope sediments: examples from Deep Sea Drilling Project cores. In: Moore, J.C. (Ed.), Structural Fabrics in Deep Sea Drilling Project Cores From Forearcs. Memoir, vol. 166. The Geological Society of America, Boulder (CO), pp. 45–54.

Knipe, R.J., 1986b. Microstructural evolution of vein arrays preserved in Deep Sea Drilling cores from the Japan Trench, Leg 57. In: Moore, J.C. (Ed.), Structural Fabrics in Deep Sea Drilling Project Cores From Forearc. Memoir, vol. 166. The Geological Society of America, Boulder (CO), pp. 75–87.

Lundberg, N., Moore, J.C., 1986. Macroscopic structural features in Deep Sea Drilling Project cores from forearc regions. In: Moore, J.C. (Ed.), Structural Fabrics in Deep Sea Drilling Project Cores From Forearcs. Memoir, vol. 166. Geological Society of America, Boulder (CO), pp. 13–44.

Maltman, A.J., Vannucchi, P., 2004. Insights from the Ocean Drilling Program on shear and fluid-flow at the mega-faults between actively converging plates. In: Alsop, G.I., Holdsworth, R.E., McCaffrey, K.J.W., Hand, M. (Eds.), Flow Processes in Faults and Shear Zones, p. 224.

Morris, J.D., et al. (2003). Proceedings of the Ocean Drilling Program, Initial Report, 205. College Station, Ocean Drilling Program.

Ranero, C.R., Grevemeyer, I., Sahling, H., Barckhausen, U., Hensen, C., Wallmann, K.,Weinrebe, W., Vannucchi, P., von Huene, R., McIntosh, K., submitted for publication. "The relationship between fluids, tectonics and seismogenesis during subduction erosion." G^3.

Saffer, D.M., Screaton, E.J., 2003. Fluid flow at the toe of convergent margins: interpretation of sharp pore-water geochemical gradients. Earth Planet. Sci. Lett. 213, 261–270.

Sammis, C.G., Biegel, R.L., 1989. Fractals, fault-gauge, and friction. Pure Appl. Geophys. 131, 255–271.

Sammis, C.G., King, G., Biegel, R., 1987. The kinematics of gouge deformation. Pure Appl. Geophys. 125, 777–812.

Sammis, C.G., Osborne, R.H., Anderson, J.L., Banerdt, M., White, P., 1986. Self-similar cataclasis in the formation of fault gauge. Pure Appl. Geophys. 124, 53–78.

Screaton, E.J., Saffer, D.M., 2005. Fluid expulsion and overpressure development during initial subduction at the Costa Rica convergent margin. Earth Planet. Sci. Lett. 233, 361–374.

Segall, P., Rice, J.R., 1995. Dilatancy, compaction, and slip instability of a fluid-infiltrated fault. J. Geophys. Res. Solid Earth 100 (B11), 22155–22171.

Sibson, R.H., 1992. Implications of fault-valve behavior for rupture nucleation and recurrence. Tectonophysics 18, 1031–1042.

Sibson, R.H., 2000. Fluid involvement in normal faulting. J. Geodyn. 29 (3–5), 469–499.

Sibson, R.H., et al., 1988. High-angle reverse faults, fluid-pressure cycling, and mesothermal gold-quartz deposits. Geology 16, 551–555.

Storti, F., Billi, A., Salvini, F., 2003. Particle size distributions in natural carbonate fault rocks: insights for non-self-similar cataclasis. Earth Planet. Sci. Lett. 206 (1–2), 173–186.

Tobin, H., Vannucchi, P., Meschede, M., 2001. Structure, inferred mechanical properties, and implications for fluid transport in the decollement zone, Costa Rica convergent margin. Geology 29 (10), 907–910.

Turcotte, D.L., 1986. Fractals and fragmentations. J. Geophys. Res. 91, 1921–1926.

Vannucchi, P., Scholl, D.W., Meschede, M., McDougall-Reid, K., 2001. Tectonic erosion and consequent collapse of the Pacific margin of Costa Rica: combined implications from ODP Leg 170, seismic offshore data, and regional geology of the Nicoya Peninsula. Tectonics 20 (5), 649–668.

Vannucchi, P., Tobin, H., 2000. Deformation structures and implications for fluid flow at the Costa Rica convergent margin, ODP Sites 1040 and 1043, Leg 170. J. Struct. Geol. 22 (8), 1087–1103.

von Huene, R., Ranero, C.R., Vannucchi, P., 2004. Generic model of subduction erosion. Geology 32 (10), 913–916.

Wang, K., Hu, Y., 2006. Accretionary prisms in subduction earthquake cycles: the theory of dynamic Coulomb wedge. J. Geophys. Res. 111, B06410. doi:10.1029/2005JB004094.